

Advancements in High Precision Decay Pion Spectroscopy of s-shell Hypernuclei at MAMI

Ryoko KINO^{1,2}, Patrick ACHENBACH³, Takeru AKIYAMA^{1,2}, Ralph BÖHM⁴, Michael O. DISTLER⁵, Philipp ECKERT⁵, Anselm ESSER⁵, Julian GERATZ⁵, Christian HELMEL⁵, Matthias HOEK⁵, Tatsuhiro ISHIGE^{1,2}, Masashi KANETA¹, Pascal KLAG⁵, Harald MERKEL⁵, Masaya MIZUNO¹, Ulrich MÜLLER⁵, Sho NAGAO⁶, Satoshi N. NAKAMURA^{6,1}, Kotaro NISHI⁶, Ken NISHIDA⁶, Kazuki OKUYAMA^{1,2}, JosefPOCHODZALLA^{5,7}, Tianhao SHAO^{5,8}, Björn Sören SCHLIMME⁵, Marcell STEINEN⁷, Koga TACHIBANA^{1,2}, Michaela THIEL⁵, and Daigo WATANABE¹
for the A1 hypernuclear collaboration

¹*Graduate School of Science, Tohoku University, Sendai, Miyagi 980-8578, Japan*

²*Graduate Program on Physics for the Universe (GP-PU), Tohoku University, Sendai, Miyagi, 980-8578, Japan*

³*Thomas Jefferson National Accelerator Facility (JLab), Newport News, Virginia 23606, USA*

⁴*Facility for Antiproton and Ion Research (FAIR), 64291 Darmstadt, Germany*

⁵*Institute for Nuclear Physics, Johannes Gutenberg University Mainz, 55099 Mainz, Germany*

⁶*Graduate School of Science, The University of Tokyo, Tokyo, 113-0033, Japan*

⁷*Helmholtz Institute Mainz, GSI Helmholtzzentrum für Schwerionenforschung, Darmstadt, Johannes Gutenberg University Mainz, 55099 Mainz, Germany*

⁸*Shanghai Research Center for Theoretical Nuclear Physics, NSFC and Fudan University, Shanghai 200438, China*

E-mail: kino.ryoko.s3@dc.tohoku.ac.jp

(Received December 31, 2024)

This proceeding presents the decay pion spectroscopy experiment at the Mainz Microtron to precisely measure the Lambda binding energy of s-shell hypernuclei, especially hypertriton ($^3_\Lambda\text{H}$). Hypertritons, as fundamental Lambda hypernuclei, offer a unique insight into the interaction between nucleons and hyperons. However, experimental uncertainty remains about the essential properties of mass and lifetime, which has attracted attention as the "Hypertriton Puzzle." The present method was established by previous research, and we actually measured the absolute Lambda binding energy of $^4_\Lambda\text{H}$ with an accuracy of better than 100 keV. In this proceeding, we explain the beam energy measurement method introduced in this experiment to reduce the systematic error by one order of magnitude compared to previous experiments and the new target system developed to ensure the yield of $^3_\Lambda\text{H}$. In addition, mention the latest analysis status.

KEYWORDS: hypertriton, Lambda-hypernucleus, binding energy, lifetime, decay pion spectroscopy, Mainz Microtron, lithium target

1. Introduction

A hypertriton ($^3_\Lambda\text{H}$) is a three-body system consisting of a proton, a neutron, and a Lambda, and is the lightest and simplest of the Lambda hypernuclei in which bound systems have been observed. The investigation of the YN interaction between hyperons and nucleons not only extends the well-understood NN interaction to the baryonic force and deepens the unified understanding, but also leads to the understanding of the physics of heavy neutron stars. $^3_\Lambda\text{H}$ can be said to be a benchmark in strangeness nuclear physics. However, despite being the most basic structure, there is still a large

experimental uncertainty about its basic properties, namely mass and lifetime. Figure 1 shows the Lambda binding energy and lifetime of ${}_{\Lambda}^3H$ summarized in the Hypernuclear Chart [1]. The Lambda

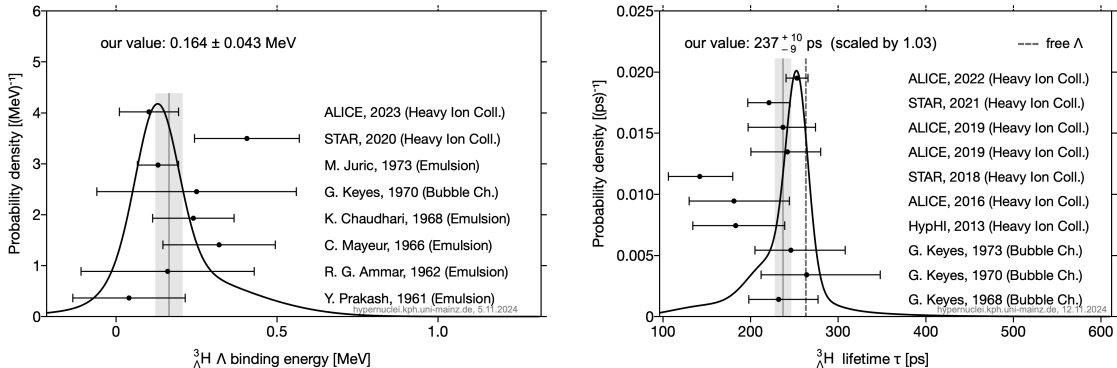


Fig. 1. Previously reported experimental data on the Lambda binding energy (left) and lifetime (right) of ${}_{\Lambda}^3H$, summarized in the Hypernuclear Chart [1].

binding energy B_{Λ} summarized by M. Jurić based on the 1960s results of several nuclear emulsion and bubble chamber measurements, is $B_{\Lambda} = 130 \pm 50$ (stat.) ± 40 (syst.) keV [2]. This value has been used as input for various theoretical calculations for nearly 50 years since then. Due to this very shallow binding energy, ${}_{\Lambda}^3H$ was understood as a picture of forming a Lambda halo nucleus, and its lifetime was predicted to be almost the same as that of a Lambda particle in free space [3]. However, in the 2010s, several heavy ion collision experimental groups, including the Hyp-HI collaboration, reported lifetime values contradicting this prediction [4–7]. The values reported were significantly shorter than the lifetime of a typical Lambda hypernucleus, $\tau \approx 200$ ps, suggesting the existence of an unknown physical interpretation. This has attracted attention as the “Hypertriton Puzzle.” In the 2020s, two heavy ion collision experiment groups, the STAR, and ALICE collaborations, reported discrepant values for B_{Λ} . The ALICE group’s value, $B_{\Lambda} = 102 \pm 63$ (stat.) ± 67 (syst.) keV [8], is roughly consistent with the past Juric value, while the STAR group’s value, $B_{\Lambda} = 406 \pm 120$ (stat.) ± 110 (syst.) keV [9], is significantly deeper. Furthermore, the systematic errors of both groups are considerable.

In light of this situation, we have reported on the A1 hypernuclear collaboration conducted an experiment to measure the Lambda binding energy of ${}_{\Lambda}^3H$ with high precision using a completely independent method called Decay Pion Spectroscopy. This technique was established through a previous experiment described in the next section, and it is possible to measure the absolute value of the binding energy with an accuracy of several tens of keV.

2. Experimental method

2.1 Principle and Apparatus

Figure 2 depicts the principle of this experiment and the experimental hall (A1 hall) with magnetic spectrometers. This experiment was conducted at Mainz Microtron C (MAMI-C) at Johannes Gutenberg University, Mainz, Germany. With the electron beam with 1.5 GeV provided by MAMI-C, a Lambda is produced electro-magnetically from one of the protons in the target material [10]. Some of the generated Lambda hypernuclei undergo nuclear fragmentation reactions and de-excitation in the target material, eventually resting in the ground state. Light lambda hypernuclei such as ${}_{\Lambda}^3H$ and ${}_{\Lambda}^4H$ then undergo two-body decays by mesonic weak decays emitting pions. At this time, the mass

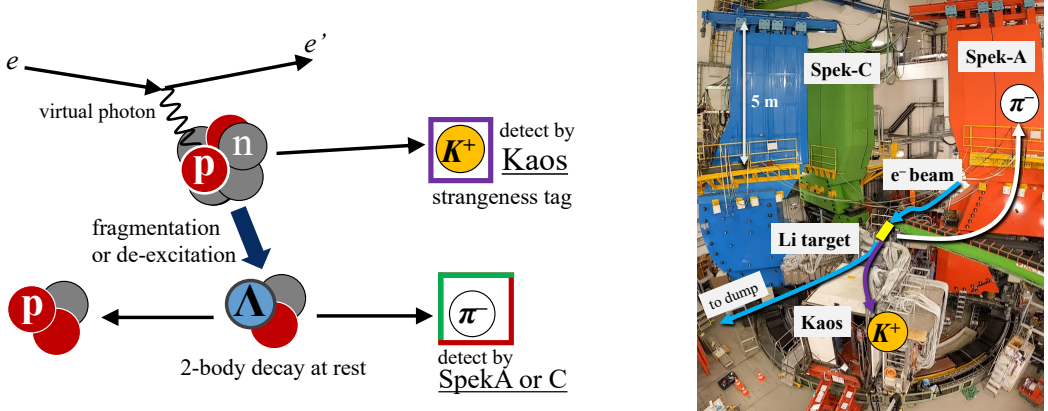


Fig. 2. Conceptual diagram showing the experimental principle (left) and a photo of the A1 hall at the Johannes Gutenberg University, Mainz where the experiment was conducted (right)

$m_{\Lambda}^A Z$) of the Lambda hypernuclei before the decay can be kinematically described by the following equation:

$$m_{\Lambda}^A Z = \sqrt{m(A(Z+1))^2 + p_{\pi^-}^2} + \sqrt{m_{\pi^-}^2 + p_{\pi^-}^2} \quad (1)$$

where $m(A(Z+1))$ is the daughter nucleus after decay, m_{π^-} is the mass of the emitted pion, and p_{π^-} is the momentum of the pion. The decay modes of ${}^3_{\Lambda} H$ and ${}^4_{\Lambda} H$ used in this experiment are as follows:



In this case, in the equation 1, the masses $m(A(Z+1))$ of the daughter nuclei ${}^3 He$ and ${}^4 He$ and the mass m_{π^-} of the pion are experimentally well-known values, the accuracy of 2.42 eV, 0.06 eV [11], and 0.35 keV [12], so the mass $m_{\Lambda}^A Z$) of the Lambda hypernucleus can be obtained by measuring the momentum p_{π^-} of the pion with high precision. The binding energy of Lambda can be calculated from the mass $m_{\Lambda}^A Z$) of the Lambda hypernucleus by the following definition:

$$B_{\Lambda} = m_{\text{core}} + m_{\Lambda} - m_{\Lambda}^A Z \quad (3)$$

Here, m_{core} is the mass of the core nucleus of the Lambda hypernucleus, and m_{Λ} is the mass of the Lambda particle. In this experiment, the measured value is only the momentum of the pion emitted by the decay, so it is possible to measure the absolute value of the binding energy with high precision.

In addition, the timing of the Kaon emitted simultaneously with the Lambda particle production is detected, and the strangeness production events are tagged, making it possible to suppress numerous background events. The Kaon tagger is performed by the dedicated spectrometer (Kaos) installed at the very forward angle (0 degree), and the momentum of the decay pions is measured by the electromagnetic spectrometers A (Spek-A) and C (Spek-C) permanently installed in the A1 hall [13]. Kaos has a dipole magnet with a wide momentum acceptance of $\pm 25\%$, and a three-layered Time of Flight (TOF) detector. The central orbit length of the dipole magnet is relatively short (6.4 m), and the design is suitable for detecting the short-lived Kaon. Spek-A and Spek-C comprise a quadrupole, a sextupole, and two dipoles, and have a large acceptance of 28 msr. The spectrometers include a vertical drift chamber (VDC) for tracking and two-layered plastic scintillator paddles (dE, TOF) for

trigger timing. The achieved momentum resolution in the previous experiment was 10^{-4} level [17]. The trigger condition in this experiment was set to:

$$\text{KAOS} \wedge (\text{SpekA} \vee \text{SpekC}) \quad (4)$$

A lithium plate was used as the target (section4).

2.2 Previous Experiment of Decay Pion Spectroscopy

A1 hyper nuclear collaboration conducted experiments using the same principle in 2012 [14] and 2014 [15], and succeeded in measuring the Lambda binding energy of ${}^4_{\Lambda}\text{H}$. The value reported in 2014 is as follows:

$$B_{\Lambda}({}^4_{\Lambda}\text{H}) = 2.157 \pm 0.005_{(\text{stat.})} \pm 0.077_{(\text{syst.})} \text{ MeV.} \quad (5)$$

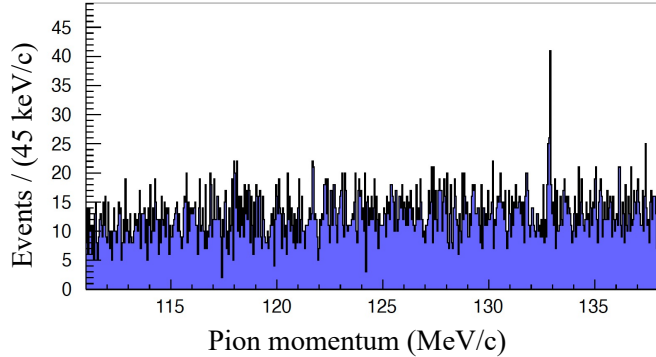


Fig. 3. Pion momentum distribution measured by Spek-A and C [16]. The clear peak seen around 133 MeV/c corresponds to the monochromatic peak of pions emitted by ${}^4_{\Lambda}\text{H}$ decay.

Figure 3 shows the momentum of pions measured by Spek-A and C, and a monochromatic peak of decay pions, as expressed by the equation 3, can be clearly seen. This peak around 133 MeV/c corresponds to the momentum of pions emitted during the decay of ${}^4_{\Lambda}\text{H}$, and by using this value, the binding energy can be obtained with a very small statistical error of 5 keV.

The systematic error is relatively large, which is due to the uncertainty of the electron beam energy (Section 3). In addition, the momentum of pions emitted during the decay of ${}^3_{\Lambda}\text{H}$ is about 114 MeV/c, which is within the range of acceptance in previous experiments, but no peak can be seen. In this experiment, ${}^9\text{Be}$ was used as the target, so it is possible that the probability of producing ${}^4_{\Lambda}\text{H}$ is overwhelmingly higher than that of ${}^3_{\Lambda}\text{H}$ during the nuclear fragmentation reaction.

In the 2022 experiment, momentum calibration was performed with a new electron beam energy measurement method using undulator interferometry to suppress systematic errors. Furthermore, a target system using lithium plates was developed to increase the probability of producing ${}^3_{\Lambda}\text{H}$ and suppress background events. Updates from previous studies incorporating these new methods will be presented in the following chapters.

3. Suppression of Systematic Error

The main cause of statistical errors is the uncertainty of the electron beam energy. This is because elastic scattering of electrons is used to perform momentum calibration with high accuracy.

Momentum calibration using elastic scattering can be performed based on the following formula:

$$\begin{aligned} \text{Momentum difference} &= p_{\text{calc}} - p_m \\ &= \sqrt{\left(\frac{E_b}{1 + E_b/M_t(1 - \cos \theta_m)} \right)^2 - m_e^2} - p_m. \end{aligned} \quad (6)$$

Where, p_m is the momentum of the elastic scattered electron measured by the spectrometer, E_b is the energy of the incident electron beam, M_t is the mass of the target nucleus, m_e is the mass of the electron, and θ_m is the measured scattering angle. ^{181}Ta , which has a relatively large mass number, was used as the target to suppress the effect of the scattering angle, and ^{12}C was used to calibrate the linearity using the scattering peaks from each excited state. Figure 4 shows an example of the

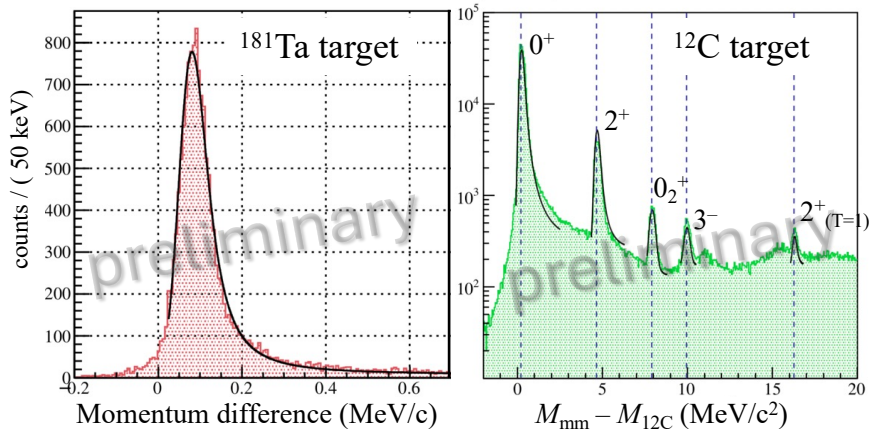


Fig. 4. Elastic scattering peaks using a ^{181}Ta target (left) and a ^{12}C target (right). Both figures were obtained in a calibration experiment conducted in the spring of 2024. The horizontal axis of the right figure is the missing mass (M_{mm}) minus the ^{12}C nucleus mass ($M_{^{12}\text{C}}$), and the energy difference between each peak is synonymous with the horizontal axis of the left figure, defined by the equation 6.

difference between the measured and calculated momentum of elastic scattered electrons obtained in a calibration experiment conducted in the spring in 2024. The fitting function used is a convolution of a Landau function with a Gaussian function, and the most probable value is used as the calibration value. For ^{181}Ta , high statistical data was obtained with a fit error of within 1 keV/c , and for ^{12}C , a peak corresponding to the 2nd 2^+ state was confirmed. The calibration method itself was established in a previous experiment, and a resolution of 10^{-4} level was achieved in that experiment.

However, in the previous experiment, the measurement method for the electron beam energy had a systematic error of $\pm 160 \text{ keV}$, and this error gave a systematic error of 77 keV to the final Lambda binding energy. In the new experiment, a novel beam energy measurement method [19] was introduced to significantly reduce this error. A conceptual diagram of this method is shown in Figure 5. Two undulators are installed on the beamline, and when an electron beam passes between them, each undulator emits synchrotron radiation. At a certain wavelength of the interference light, the Lorentz factor of the electron is calculated by measuring the interference intensity while varying the distance between the two undulators. In a proof-of-principle experiment of this method, it was demonstrated that the beam energy can be measured with a total error of $\Delta E/E \approx 18 \text{ keV}$, which is about one-tenth of the error of conventional methods [19]. In a calibration experiment conducted in the spring of 2024, it was successful for the first time in combining the electron elastic scattering

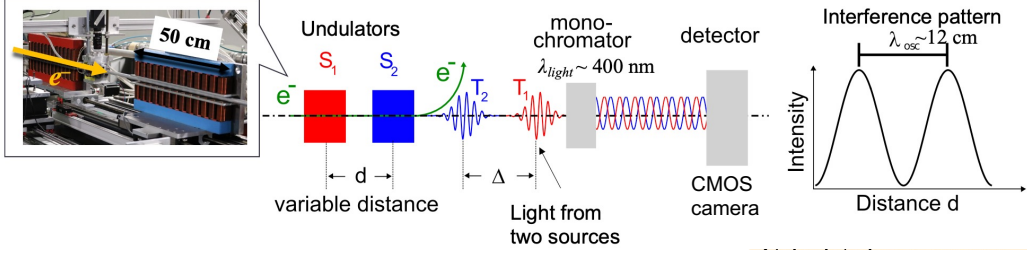


Fig. 5. Conceptual diagram of the beam energy measurement method using undulator interferometry [19]. The interference light intensity is measured by a CMOS camera while changing the distance d between two undulators S_1 and S_2 installed on the beamline, and the intensity change pattern shown on the right is obtained.

experiment and the beam energy measurement experiment using an undulator while switching the electron beam path. By combining this with the new method, it is expected that the systematic error of the binding energy can be suppressed to less than 10 keV.

4. New Lithium Targeting System for ${}^3_{\Lambda}\text{H}$ Detection

The second update from the previous experiment is the introduction of a target system using lithium (not enriched) [17, 18]. Compared to ${}^9\text{Be}$ used in the previous experiment, lithium can suppress background events generated by other hypernuclear fragment candidates with decay pion momentum close to that of ${}^3_{\Lambda}\text{H}$, such as ${}^8_{\Lambda}\text{He}$. However, it is not easy to handle because of its low density and low melting point. For these difficulties, the introduced target system's conceptual diagram and an actual photo are shown in Figure 6. To ensure a high yield while the low density, the target plate was

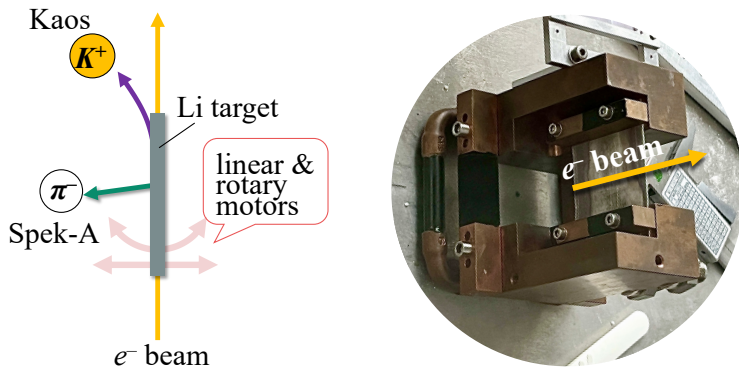


Fig. 6. Conceptual diagram of the lithium target (left) and actual photo (right). Kaons are emitted in the forward direction, while pions emitted by hypernuclear decay measured by Spek-A and C are emitted in the direction of about 90 degrees. In the photo on the right, the brown metal part has the cooling water pipes, and the actual lithium plate is installed in the center.

set along the beam direction. The geometrical width of the target was 0.75 mm for an electron beam of $\sigma \approx 0.3$ mm, and the thickness was 45 mm long. To pass the electron beam through such a long and narrow target, the spectrometer's single rate was monitored to be constant. The electron beam position was also controllable in mm increments, and the target was mounted on automatic motors

that could move it laterally and rotate, so it was always under control. As a result, the target's material thickness was $2,403 \text{ mg/cm}^2$, about 100 times larger than that of the previous experiment, ${}^9\text{Be}$: 27 mg/cm^2 . To address the low melting point, the ladder that attached the target plate was equipped with a pipe to run cooling water through it.

5. Latest Status of the Experiment and Analysis

A commissioning run was conducted in the summer of 2022, and an experiment to obtain physics data was conducted in the fall of the same year. The total runtime was 541 hours, and the beam charge was 1.08 C. In the spring of 2024, the electron elastic scattering experiment for momentum calibration and the beam energy measurement using undulator interferometry were conducted. In this experiment, data sets were taken at more than 10 times the data points of the previous experiment to cover a wide momentum range.

The analysis is currently underway. Figure 7 shows the plot of the time difference of coincidence events between Kaos and Spek-A after particle identification based on the data obtained by Kaos (left figure), and the momentum distribution of pions obtained by Spek-A (right figure). In the coincidence

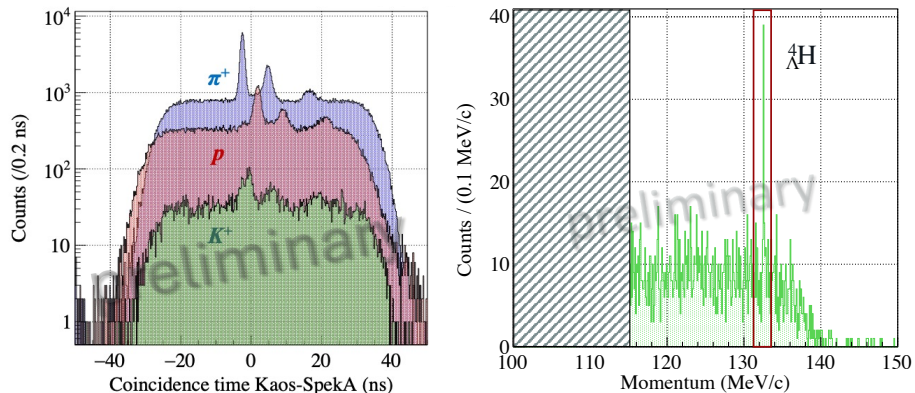


Fig. 7. The coincidence time distribution of the Kaon tagger spectrometer Kaos and the decay pion spectrometer Spek-A (left) and the momentum distribution of pions obtained by Spek-A (right). The left figure is after particle identification using the Kaos data. The clear peak seen on the right corresponds to the decay pion of ${}^4\text{H}$. The decay pion peak of ${}^3\text{H}$ has been confirmed in the meshed area.

time distribution, the timing difference due to the mass difference of each particle can be confirmed. The kaon event shown in green is the strangeness production event, and by selecting the region of this main peak, hypernuclear events can be selectively observed. The yield that can be determined at this point is almost the same as in the previous experiment. Looking at the pion momentum distribution obtained by Spek-A after selecting this peak (Figure 7 right), a monochromatic peak of the decay pion of ${}^4\text{H}$ is significantly visible. In the meshed region on the left, there is a monochromatic peak of the decay pion of ${}^3\text{H}$. This momentum distribution cannot be made public yet because a detailed analysis of particle identification is currently ongoing.

Figure 8 shows a Gaussian function fitted to the peak of the decay pion of ${}^4\text{H}$ shown in the right part of Figure 7. The value of the pion momentum obtained from this fit is $p_{\pi^-} = 132.538 \pm 0.008 \text{ MeV/c}$, which is the same statistical error as in previous studies, and the peak width was found to be $\sigma \approx 0.045 \pm 0.014 \text{ MeV/c}$. This absolute value will be updated in future analysis of momentum calibration experiment data.

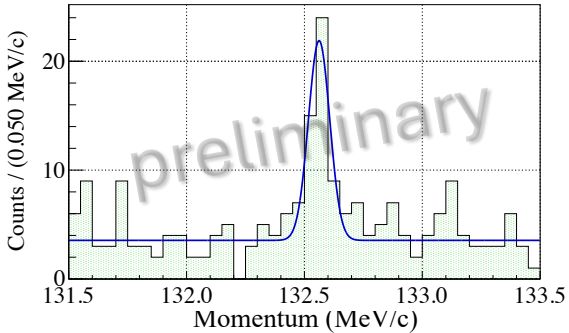


Fig. 8. The result of fitting a Gauss function to the decay pion peak of ${}^4\Lambda\text{H}$ in Figure 7.

6. Summary

In this proceeding, we reported on the principle of the experiment using Decay Pion Spectroscopy to measure the Lambda binding energy (B_Λ) of hypertritons (${}^3\Lambda\text{H}$) with high precision, updates from previous experiments, and progress on the experiment and analysis. With this method, it is possible to measure the absolute value of B_Λ with an accuracy of several tens of keV. In order to reduce systematic errors compared to previous experiments that measured the B_Λ of ${}^4\Lambda\text{H}$ with an accuracy of less than 100 keV, we introduced a beam energy measurement method using undulator interferometry. This is expected to reduce systematic errors caused by beam energy uncertainty to within 10 keV. In addition, to increase the yield of ${}^3\Lambda\text{H}$, we developed a target system using lithium plates. The problems of low density and low melting point were solved by a configuration that keeps the material thickness 100 times larger.

The experiment was conducted in 2022, and the ${}^4\Lambda\text{H}$ yield was similar to that of previous experiments. The analysis is currently underway, and current particle identification has shown a clear peak for ${}^4\Lambda\text{H}$. A significant peak has also been confirmed for ${}^3\Lambda\text{H}$. Further detailed analysis will provide more precise particle identification and momentum calibration using the results of undulator interferometry data analysis. This study aims to provide updated values for B_Λ that could address long-standing discrepancies in hypertriton measurements and deepen our understanding of the strangeness nuclear physics.

Acknowledgements

This project is supported by the Deutsche Forschungsgemeinschaft, Grant Number PO256/7-1, and the European Union's Horizon 2020 research and innovation program No. 824093. The work is partially supported by JSPS KAKENHI Grant Numbers JP18H05459, 18H01219, 17H01121, 120002001, 15684005, 16GS0201, and Grant-in-Aid for JSPS Fellows, Japan Number 23KJ0180. Three of the authors (RK, KO, and KT) acknowledge support from the JSPS Research Fellowship for Young Scientists, Japan, and five of the authors (RK, TA, TI, KO, and KT) are supported by the Graduate Program on Physics for the Universe (GP-PU), Tohoku University. The presented data were partly collected within the framework of the PhD thesis of Ryoko Kino at Tohoku University.

References

- [1] P. Eckert *et al.*, *Chart of hypernuclides – Hypernuclear structure and decay data* (2021)
- [2] M. Jurić *et al.*, Nucl. Phys. B **52**, 1 (1973) 1-30.
- [3] H. Kamada *et al.*, Phys. Rev. C **57**, 4 (1998).

- [4] C. Rappold *et al.*, Nucl.Phys. A **913** (2013) 170-184.
- [5] L. Adamczyk *et al.*, Phys.Rev.C **97** (2018) 5, 054909.
- [6] STAR Collaboration, Science **328** (2010) 58.
- [7] J. Adam *et al.*, Phys. Lett. B **754** (2016) 360-372.
- [8] S. Acharya *et al.*, Phys. Rev. Lett. **131** (2023) 102302.
- [9] STAR Collaboration, Nat. Phys. **16** (2020) 4, 409-412.
- [10] P. Achenbach *et al.*, Nucl. Phys. A **881** (2012) 187-198.
- [11] G. Audi *et al.*, Nucl. Phys. A **729** (2003) 337.
- [12] J. Beringer *et al.*, Phys. Rev. D **86** (2012) 010001.
- [13] K. I. Blomqvist *et al.*, Nucl. Instrum. Methods Phys. Res., Sect. A **403** (1998) 263-301.
- [14] A. Esser, S. Nagao, F. Schulz *et al.*, Phys. Rev. Lett. **114** (2015) 232501.
- [15] F. Schulz *et al.*, Nucl. Phys. A **954** (2016) 149.
- [16] F. Schulz, Ph.D. thesis, Johannes Gutenberg-Universität, Mainz (2016)
- [17] P. Achenbach *et al.*, Nucl. Instrum. Methods Phys. Res., Sect. A **1043** (2022) 167500.
- [18] P. Eckert, Ph.D. thesis, Johannes Gutenberg-Universität, Mainz (2023)
- [19] P. Klag *et al.*, Nucl. Instrum. Methods Phys. Res., Sect. A **910** (2018) 147-156.